

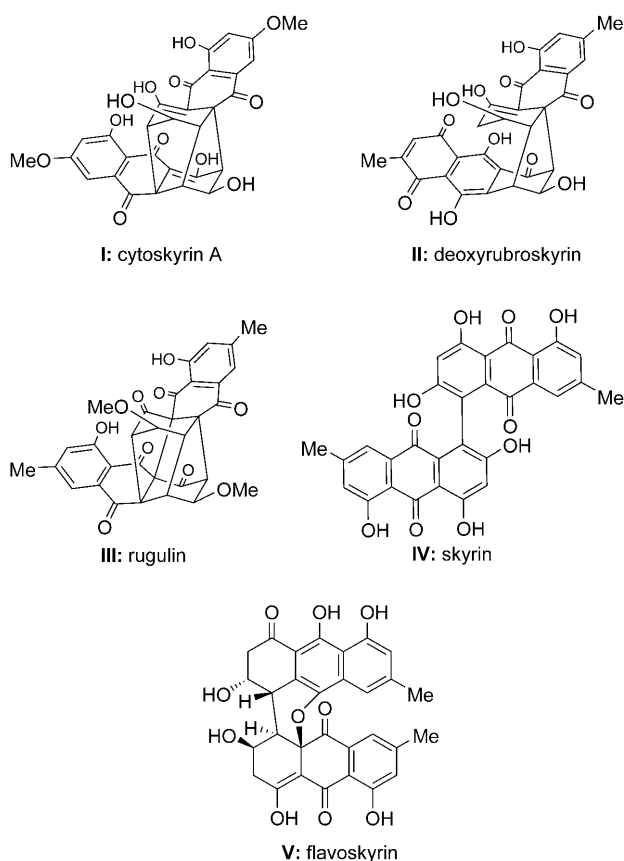
DOI: 10.1002/ange.200502011

**The Cytoskyrin Cascade: A Facile Entry into Cytoskyrin A, Deoxyrubroskyrin, Rugulin, Skyrin, and Flavoskyrin Model Systems\*\****K. C. Nicolaou,\* Charles D. Papageorgiou, Jared L. Piper, and Raj K. Chadha*

The collection of naturally occurring compounds shown in Scheme 1 (**I**: cytoskyrin A,<sup>[1]</sup> **II**: deoxyrubroskyrin,<sup>[2a]</sup> **III**: rugulin,<sup>[3]</sup> **IV**: skyrin,<sup>[2b,4]</sup> and **V**: flavoskyrin<sup>[2a]</sup>) represents a growing class of natural products often referred to as bisanthraquinones. Notable among them are cytoskyrin A,<sup>[1]</sup> the newest member of the class whose striking biological activity includes potency down to 12.5 ng mL<sup>-1</sup> in the biochemical induction assay (BIA), and rugulin, whose structural motif exhibits the highest strain of them all. Isolated from small-scale cultures of the endophytic fungus CR200 (*Cytospora* sp.), which were collected from a branch of a *Conocarpus erecta* tree in the Guanacaste Conservation area of Costa Rica, cytoskyrin A (**I**) presents a challenging synthetic target by virtue of its cage-like structural motif, as do its siblings whose more (**III**) or less (**II** and **V**) enclosed cages are defined by the number of bonds linking their two

[\*] Prof. Dr. K. C. Nicolaou, Dr. C. D. Papageorgiou, Dr. J. L. Piper, Dr. R. K. Chadha  
Department of Chemistry and  
The Skaggs Institute for Chemical Biology  
The Scripps Research Institute  
10550 North Torrey Pines Road, La Jolla, CA 92037 (USA)  
Fax: (+1) 858-784-2469  
E-mail: kcn@scripps.edu  
and  
Department of Chemistry and Biochemistry  
University of California, San Diego  
9500 Gilman Drive, La Jolla, CA 92093 (USA)

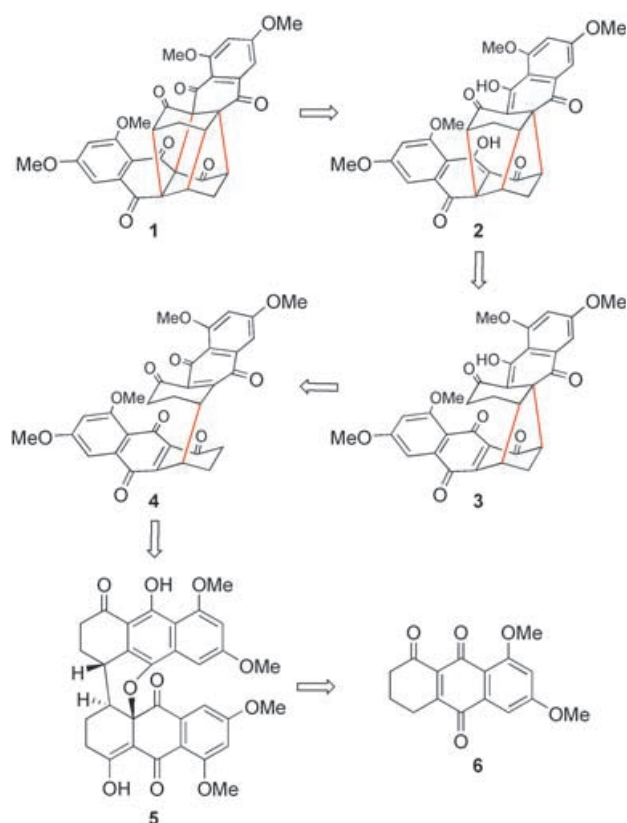
[\*\*] We thank Prof. Albert Eschenmoser for stimulating discussions and Dr. D. H. Huang and Dr. G. Siuzdak for NMR spectroscopic and mass spectrometric assistance, respectively. Financial support for this work was provided by grants from the National Institutes of Health (USA) and the Skaggs Institute for Chemical Biology, and a postdoctoral fellowship from the George E. Hewitt Foundation (to J.L.P.).



**Scheme 1.** Naturally occurring modified bisanthraquinones.

anthraquinone monomeric units. Herein we report the construction of model systems for all five natural products I–V, namely compounds 1–5, respectively, from anthraquinone 6 (Scheme 2) through a stepwise or a cascade sequence of reactions, herein coined the “cytoskyrin cascade”.

The present investigations were inspired by the novel molecular architectures of the targeted natural products (Scheme 1) and the work of Shibata and co-workers.<sup>[2]</sup> To scout possible routes to these intriguing structures, the model systems 1–5 (Scheme 2) were selected as initial targets. The complexity of these molecules decreases as we move from 1 (whose anthraquinone units are held together by four carbon–carbon bonds) to 4 (which is cojoined by only one single bond). The origins of 4 can be traced retrosynthetically to 6 through a dimerization process that may or may not proceed via dimer 5, as shown below.<sup>[5]</sup> Before we reveal our pathway to these model systems, however, a further comment concerning the cage-like core structure of 1<sup>[6]</sup> is in order. This novel core structure presented by the parent C<sub>12</sub>H<sub>16</sub> hydrocarbon VI (Figure 1), named herein “skyrane”, is walled by two slightly distorted six-membered rings (forming the top and bottom of a tilted hexagonal capsule) and four uniformly twisted five-membered rings, leading to a considerably strained architecture. As the bonds are removed one by one from this aesthetically appealing capsule, the strain associated with each daughter molecule is expected to decrease. In terms of a synthetic barrier, however, this trend is counterbalanced



**Scheme 2.** Model systems (1–5) of the bisanthraquinone natural products rugulin, cytoskyrin, deoxyrubroskyrin, skyrin, and their potential precursor anthraquinone monomer.

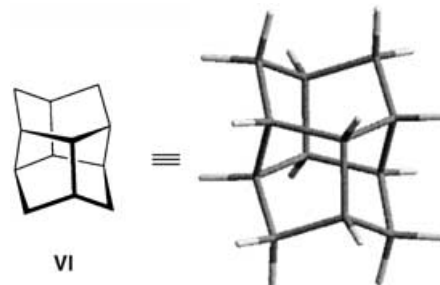
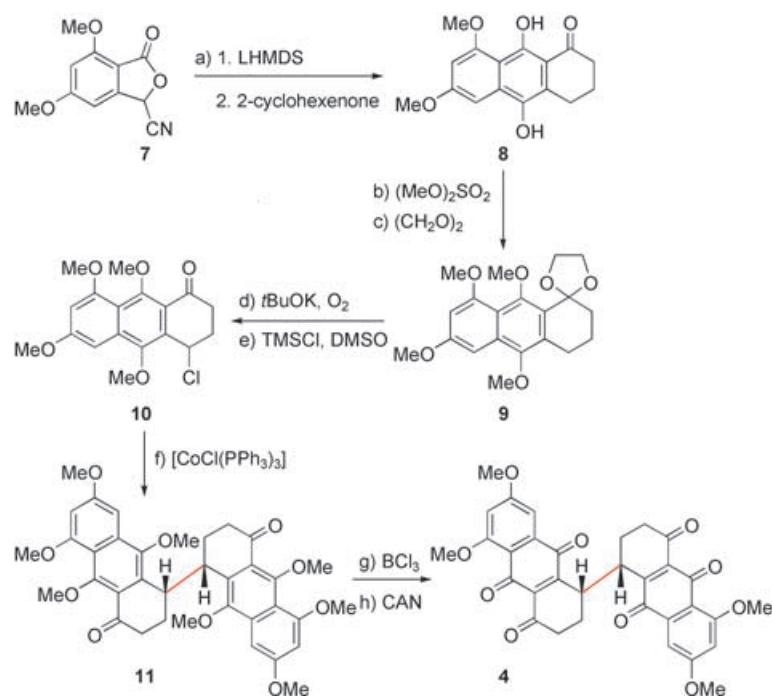


**Figure 1.** Parent C<sub>12</sub>H<sub>16</sub> hydrocarbon, “skyrane”.

by entropy: as the cage is being built, proximity should favor the next bond formation.

Scheme 3 summarizes the synthesis of the first model system, bisanthraquinone 4, through a sequence that features a Hauser annulation<sup>[7]</sup> to construct the requisite tricyclic system and a radical dimerization to provide the required hexacyclic compound. Thus, treatment of nitrile 7 with LHMDs in THF at –78°C, followed by addition of 2-cyclohexenone (–78→25°C) gave crude anthradihydroquinone 8, which was directly subjected to methylation and dioxolane formation to afford protected compound 9 in 58% overall yield for the three steps. A subsequent benzylic oxygenation/chlorination sequence then converted 9 into 10 in 57% overall yield. The anticipated dimerization of 10 was



**Scheme 3.** a) **7** (1.1 equiv), THF, LHMS (1.5 equiv),  $-78^{\circ}\text{C}$ ; then 2-cyclohexenone (1.0 equiv)  $-78 \rightarrow 25^{\circ}\text{C}$ , 4 h; b)  $(\text{MeO})_2\text{SO}_2$  (5.0 equiv),  $\text{K}_2\text{CO}_3$  (5.0 equiv), acetone, reflux, 12 h; c) ethylene glycol (2.0 equiv), benzene, PPTS (0.2 equiv), reflux, 24 h, 58% over three steps; d)  $t\text{BuOK}$  (6.0 equiv),  $\text{O}_2$ , DMSO, 2 h; e) TMSI (2.0 equiv), DMSO, 10 min, 57% over two steps; f)  $[\text{CoCl}(\text{PPh}_3)_3]$  (1.2 equiv), benzene,  $25^{\circ}\text{C}$ , 3 h; g)  $\text{BCl}_3$  (2.2 equiv),  $\text{CH}_2\text{Cl}_2$ ,  $-78 \rightarrow 25^{\circ}\text{C}$ , 12 h; h) CAN (4.0 equiv),  $\text{CH}_3\text{CN}/\text{H}_2\text{O}$  1:1, 10 min, 50% over two steps. CAN = cerium ammonium nitrate; DMSO = dimethyl sulfoxide; LHMS = lithium hexamethyldisilazide; PPTS = pyridinium *p*-toluenesulfonate; TMS = trimethylsilyl.

performed by exposure to  $[\text{CoCl}(\text{PPh}_3)_3]$ <sup>[8]</sup> in benzene at  $25^{\circ}\text{C}$ , leading, through radical species, to the desired *dl* dimer (**11**) as the major product (55% yield) accompanied by its *meso* isomer (25%). The two isomers were separated by silica-gel flash chromatography and unambiguously identified through X-ray crystallographic analysis of a later intermediate (see below). The two methyl groups residing on the oxygen atoms nearest to the carbonyl moieties were then selectively cleaved from the major isomer **11** by exposure to  $\text{BCl}_3$  in  $\text{CH}_2\text{Cl}_2$  at  $-78^{\circ}\text{C}$  to furnish the corresponding diphenolic compound, whose oxidation with CAN resulted in the formation of the targeted *dl* bisanthraquinone **4** (50% overall yield for the two steps). Compound **4** crystallized in suitable form for X-ray crystallographic analysis (see ORTEP drawing,<sup>[9]</sup> Figure 2), which confirmed its stereochemical identity and that of its progenitor, compound **11**.

A second pathway to the bisanthraquinone **4** was devised from monoquinone **6**, obtained in quantitative yield by oxidation of hydroquinone **8** with CAN. Thus, exposure of **6** to catalytic amounts of CSA in  $\text{CH}_2\text{Cl}_2$  at  $25^{\circ}\text{C}$  for 1 h resulted in the formation of the flavoskyrin model system **5** (94% yield) through dimerization of the enol form **12** of the starting material (**6**  $\rightarrow$  **5**) could be brought about by a catalytic amount of a mild base (e.g.  $i\text{Pr}_2\text{NEt}$ ) in 90% yield. This highly efficient dimerization is presumed to proceed either through a Diels–Alder-type<sup>[2c,f]</sup>

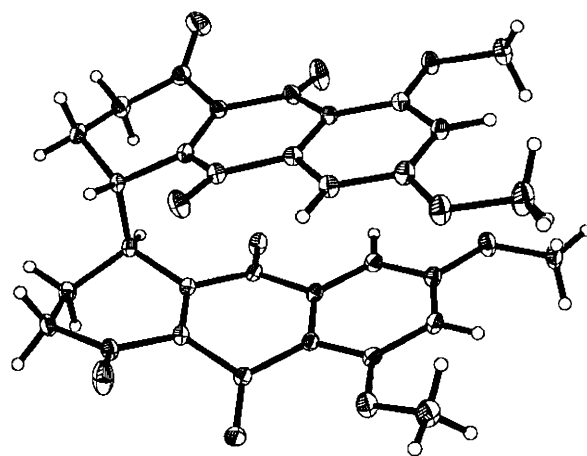
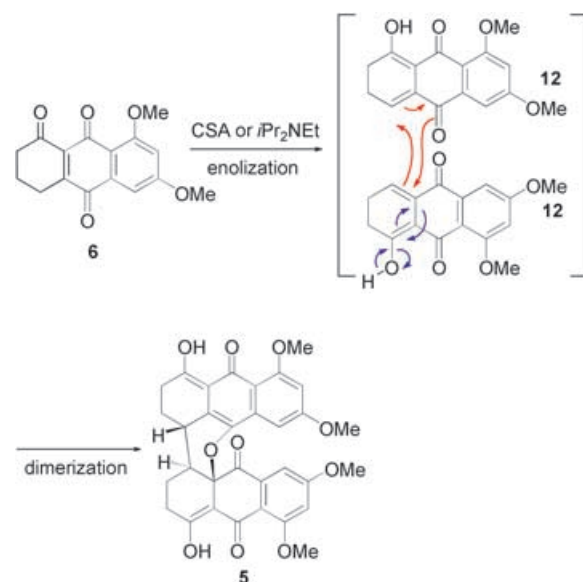


**Figure 2.** ORTEP drawing of structure **4** (drawn at the 30% probability level).

reaction, or through a double Michael reaction, as shown in Scheme 4. The structure of dimer **5** was confirmed by X-ray crystallographic analysis (see ORTEP drawing,<sup>[9]</sup> Figure 3). Oxidation of **5** with  $\text{MnO}_2$  (presumably through the mechanism shown in Scheme 5, structure **VII**) then furnished the desired *dl* bisanthraquinone **4** in 83% yield (Scheme 6). Remarkably, bisanthraquinone **4** was converted into the deoxyrubroskyrin model system **3** in 65% yield simply by exposure to  $\text{Et}_3\text{N}$  (2.0 equiv) in  $\text{CH}_2\text{Cl}_2$  at  $25^{\circ}\text{C}$  for 1 h.<sup>[2a,e,f]</sup> Even more impressive was the conversion of **3** into the cytoskyrin model structure **2** (95% yield), a process that required longer exposure to  $\text{Et}_3\text{N}$  (5.0 equiv) and slightly higher temperature (16 h,  $45^{\circ}\text{C}$ ). This latter transformation (**3**  $\rightarrow$  **2**) could also be accomplished under acidic conditions, albeit in lower yield (PPTS, 2.0 equiv, toluene, 24 h,  $100^{\circ}\text{C}$ , 65%). Finally, the cytoskyrin-type



**Scheme 4.** Postulated mechanism for the dimerization of tricyclic quinone **6**, through enolization and a Diels–Alder or double Michael reaction. CSA = ( $\pm$ )-10-camphorsulfonic acid.

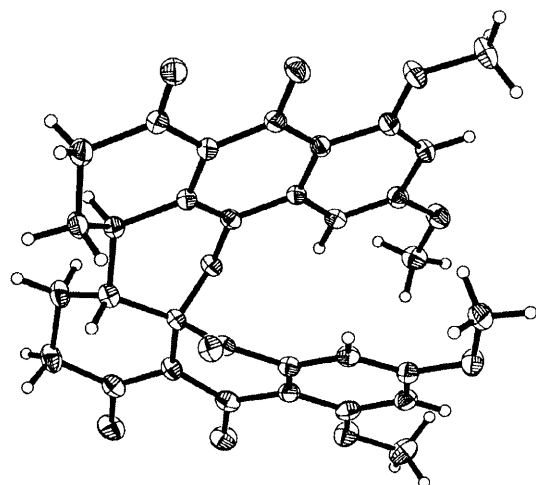
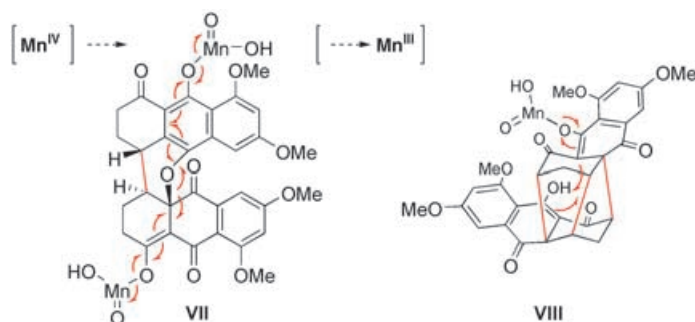


**Figure 3.** ORTEP drawing of structure **5** (drawn at the 30% probability level).

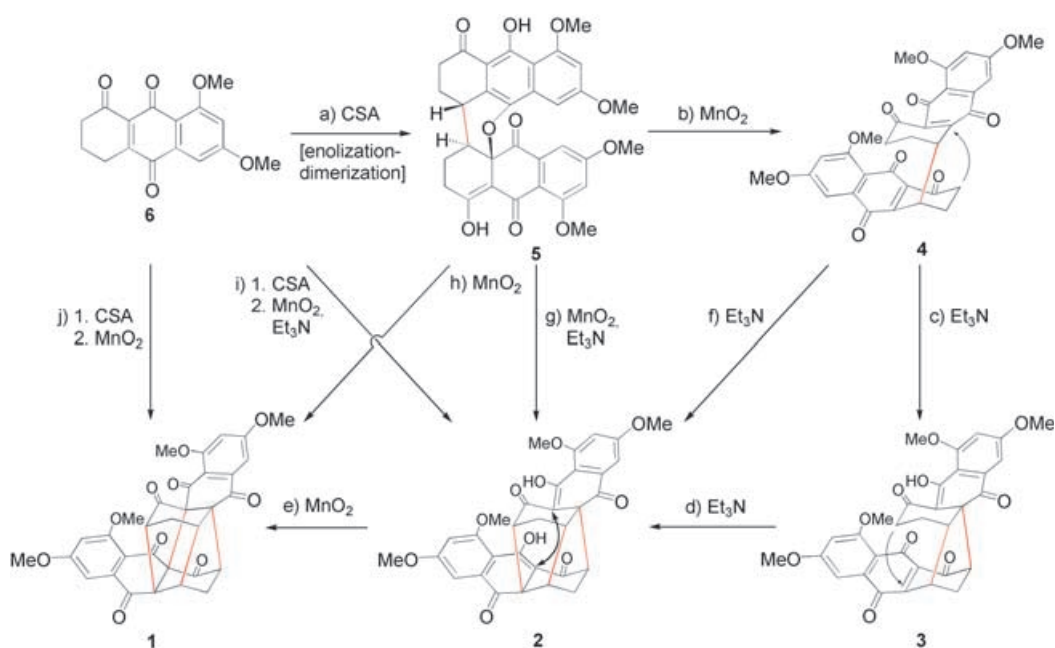
compound **2** was transformed into the rugulin-type structure **1** (Table 1) in 95% yield simply by exposure to  $\text{MnO}_2$ <sup>[2a]</sup> through an oxidation process that also involved a carbon–carbon bond formation (see Scheme 5, structure **VIII** for a presumed mechanism).

Remarkable as these individual steps may be, they were aesthetically surpassed by the beauty of a number of cascade sequences developed in these studies (Scheme 6). The fact that only a mild base was required to carry out the double Michael reaction leading to **2** (**4**→**3**→**2**; Table 1) and the suspicion that  $\text{MnO}_2$  contained such basic species prompted us to attempt this cascade with  $\text{MnO}_2$  as the only reagent. Indeed, on exposure to freshly prepared  $\text{MnO}_2$  in  $\text{CH}_2\text{Cl}_2$ , compound **5** (Table 1) was transformed into **1** in quantitative yield,<sup>[10]</sup> through the intermediacy of **4**, then **3**, and finally **2**, all of which were observed by TLC analysis (cascade **5**→**1**; excess  $\text{MnO}_2$ , 48 h, 45°C). Interestingly, addition of  $\text{Et}_3\text{N}$  (10.0 equiv) to the starting reaction mixture (**5**,  $\text{MnO}_2$ ) and heating to 45°C for 20 h resulted in the exclusive formation of **2** (in quantitative yield), with  $\text{Et}_3\text{N}$  apparently inhibiting the last oxidation step (**2**→**1**, presumably through slow deactivation of the  $\text{MnO}_2$ ). Even more impressive was the five-step cascade sequence involving the transformation of the tricyclic mon-



**Scheme 5.** Postulated mechanism for the  $\text{MnO}_2$  oxidation of compound **5** to **4** (**VII**) and **2** to **1** (**VIII**). This working hypothesis depiction is not based on experimental evidence and is not meant to exclude any other mechanism. The proximity of the  $\text{Mn}=\text{O}$  and enol groups within **VIII** bodes well for an intramolecular interaction between them as part of the mechanism.

omer **6** into the nonacyclic cytoskyrin model system **2** in 66% yield<sup>[10]</sup> (cascade **6**→**2**). The latter cascade required treatment of **6** with CSA (0.125 equiv) in  $\text{CH}_2\text{Cl}_2$  for 1 h at 25°C, conditions that led to the formation of **5** as indicated by TLC analysis, followed by addition of  $\text{MnO}_2$  (excess) and  $\text{Et}_3\text{N}$  (10.0 equiv) and heating to 45°C with stirring for 36 h, to afford the cytoskyrin model system **2**, through the intermediacy of the fleeting compounds **4** and **3**. This remarkable cascade encompasses an enolization step, followed by a stereoselective dimerization reaction, an oxidation, and finally, an intramolecular double Michael sequence. A similar



**Scheme 6.** The cytoskyrin cascade: synthesis of flavoskyrin-, skyrin-, deoxyrubsoskyrin-, cytoskyrin-, and rugulin-type structures from anthraquinone **6**. All steps can be carried out sequentially in one pot or can be stopped at any stage. Reagents and conditions: a) CSA (0.125 equiv),  $\text{CH}_2\text{Cl}_2$ , 25°C, 1 h, 94%; b)  $\text{MnO}_2$  (10.0 equiv),  $\text{CH}_2\text{Cl}_2$ , 25°C, 1 h, 83%; c)  $\text{Et}_3\text{N}$  (2.0 equiv),  $\text{CH}_2\text{Cl}_2$ , 1 h, 25°C, 65%; d)  $\text{Et}_3\text{N}$  (5.0 equiv),  $\text{CH}_2\text{Cl}_2$ , 16 h, 45°C, 95%; e)  $\text{MnO}_2$  (10.0 equiv),  $\text{CH}_2\text{Cl}_2$ , 25°C, 20 h, 95%; cascade sequences: f) **4**→**2**,  $\text{Et}_3\text{N}$  (5.0 equiv),  $\text{CH}_2\text{Cl}_2$ , 16 h, 45°C, 95%; g) **5**→**2**,  $\text{MnO}_2$  (10.0 equiv),  $\text{Et}_3\text{N}$  (5.0 equiv),  $\text{CH}_2\text{Cl}_2$ , 20 h, 25→45°C, 100%; h) **5**→**1**,  $\text{MnO}_2$  (10.0 equiv),  $\text{CH}_2\text{Cl}_2$ , 48 h, 45°C, 100%; i) **6**→**2**, CSA (0.125 equiv),  $\text{CH}_2\text{Cl}_2$ , 1 h, 25°C; then  $\text{MnO}_2$  (10.0 equiv),  $\text{Et}_3\text{N}$  (10.0 equiv), 36 h, 45°C, 66%; j) **6**→**1**, CSA (0.125 equiv),  $\text{CH}_2\text{Cl}_2$ , 1 h, 25°C; then  $\text{MnO}_2$  (10.0 equiv), 88 h, 25°C, 75%.



experiment in which no Et<sub>3</sub>N was added resulted in a six-step cascade transforming **6** to rugulin model system **1** in an impressive 75 % yield.

X-ray crystallographic analysis of compound **3**<sup>[9]</sup> revealed an interesting phenomenon, reminiscent of the classic observation of Ermer with secododecahedrane.<sup>[11]</sup> As in that case, our initial analysis led to a symmetrical structure (see ORTEP drawing, Figure 4 a), an architecture that was contradicted by

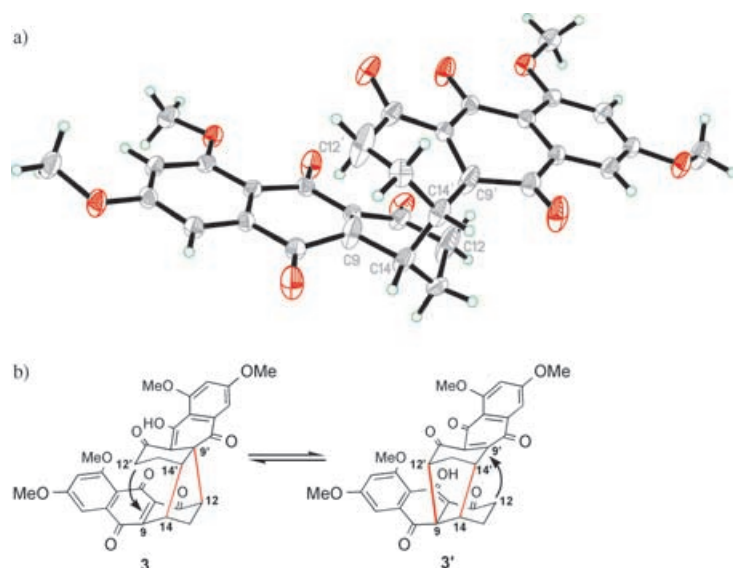


**Figure 4.** ORTEP drawing of compound **3** (drawn at the 30% probability level) obtained by X-ray crystallographic analysis (using C2/c space group) at ambient temperature and possible equilibration of **3** and **3'**.

<sup>1</sup>H NMR spectroscopy, which revealed a nonsymmetrical structure for the molecule.<sup>[12]</sup> This rare observation may be due to crystal disorder,<sup>[13]</sup> or dynamic equilibrium involving a two-proton shuttle in which the C12–C9' bond within **3** breaks as the C12'–C9 bond within **3'** forms (**3**→**3'**, Figure 4b). The structures **3** and **3'** are identical, and X-ray crystallographic analysis reveals an average picture with bond lengths C12–C9' = C12'–C9 = 2.372 Å and C14–C14' = 1.56 Å.<sup>[14]</sup>

The described chemistry provides easy and efficient access to a variety of molecular architectures representing the core structures of numerous natural products, underscoring at the same time the importance of cascade sequences in complex molecule construction. Our experience with the X-ray crystallographic analysis of the deoxyrubroskyrin-type compound **3** should serve as a reminder of the occasional hazards posed by dynamic and/or crystal-disorder phenomena in the solid state and their impact on structure elucidation. While the total synthesis of several members of the bisanthraquinone family of compounds shall now be forthcoming, the gauntlet thrown by skyrane **VI** (Figure 1) is also begging for a solution, a challenge that has not escaped our attention.

Received: June 10, 2005

Published online: August 25, 2005

**Table 1:** Selected physical properties for **1**–**5**.

<p><b>1:</b> <math>R_f</math> = 0.53 (CH<sub>2</sub>Cl<sub>2</sub>/MeOH 10:1); <sup>1</sup>H NMR (500 MHz, CDCl<sub>3</sub>): <math>\delta</math> = 6.99 (2 H, d, <math>J</math> = 2.0 Hz), 6.80 (2 H, d, <math>J</math> = 2.0 Hz), 3.95 (6 H, s), 3.91 (6 H, s), 3.39 (2 H, br), 3.08 (2 H, d, <math>J</math> = 8.0 Hz), 2.82 (2 H, dd, <math>J</math> = 13.0, 9.0 Hz), 2.28 ppm (2 H, d, <math>J</math> = 13.0 Hz); <sup>13</sup>C NMR (175 MHz, CDCl<sub>3</sub>): <math>\delta</math> = 201.9, 194.7, 186.9, 164.2, 159.8, 137.8, 122.2, 106.5, 101.4, 74.5, 66.2, 57.0, 56.8, 56.6, 56.0, 39.2 ppm; IR (film): <math>\tilde{\nu}_{max}</math> = 1748, 1684, 1654, 1590, 1560, 1458, 1320, 1236 cm<sup>-1</sup>; HRMS (ESI TOF) (<math>m/z</math>): calcd for C<sub>32</sub>H<sub>25</sub>O<sub>10</sub><sup>+</sup>: 569.1442 [M+H]<sup>+</sup>; found: 569.1420</p> <p><b>2:</b> <math>R_f</math> = 0.80 (CH<sub>2</sub>Cl<sub>2</sub>/MeOH 10:1); <sup>1</sup>H NMR (500 MHz, CDCl<sub>3</sub>): <math>\delta</math> = 15.90 (2 H, s), 7.24 (2 H, d, <math>J</math> = 2.5 Hz), 6.77 (2 H, d, <math>J</math> = 2.5 Hz), 3.95 (6 H, s), 3.94 (6 H, s), 3.66 (2 H, br), 2.89 (2 H, d, <math>J</math> = 6.0 Hz), 2.13 (2 H, dd, <math>J</math> = 12.0, 6.0 Hz), 1.65 ppm (2 H, d, <math>J</math> = 12.0 Hz); <sup>13</sup>C NMR (125 MHz, CDCl<sub>3</sub>): <math>\delta</math> = 197.6, 196.5, 173.0, 164.5, 161.8, 135.0, 114.4, 105.6, 104.0, 103.7, 57.8, 57.4, 56.8, 56.0, 48.1, 30.0 ppm; IR (film): <math>\tilde{\nu}_{max}</math> = 2932, 1617, 1574, 1315, 1039, 909, 731 cm<sup>-1</sup>; HRMS (ESI TOF) (<math>m/z</math>): calcd for C<sub>32</sub>H<sub>27</sub>O<sub>10</sub><sup>+</sup>: 571.1599 [M+H]<sup>+</sup>; found: 571.1585</p> <p><b>3:</b> <math>R_f</math> = 0.45 (CH<sub>2</sub>Cl<sub>2</sub>/MeOH 10:1); <sup>1</sup>H NMR (500 MHz, CDCl<sub>3</sub>): <math>\delta</math> = 16.0 (1 H, s), 7.21 (1 H, d, <math>J</math> = 2.0 Hz), 7.05 (1 H, d, <math>J</math> = 2.5 Hz), 6.78 (1 H, d, <math>J</math> = 2.5 Hz), 6.76 (1 H, d, <math>J</math> = 2.5 Hz), 4.00 (3 H, s), 3.98 (1 H, d, <math>J</math> = 5.5 Hz), 3.96 (3 H, s), 3.93 (3 H, s), 3.92 (3 H, s), 3.87 (1 H, br), 3.18 (1 H, d, <math>J</math> = 3.5 Hz), 2.13–2.05 ppm (1 H, m), 2.05–1.90 (3 H, m), 1.90–1.80 (1 H, m), 1.80–1.78 (1 H, m); <sup>13</sup>C NMR (125 MHz, CDCl<sub>3</sub>): <math>\delta</math> = 196.1, 195.4, 186.1, 186.4, 179.5, 179.3, 164.8, 164.4, 162.6, 161.7, 156.2, 136.6, 134.7, 130.8, 116.1, 115.1, 105.7, 105.4, 104.3, 103.6, 102.6, 60.3, 57.1, 56.9, 56.5, 56.0, 55.9, 39.9, 39.6, 36.1, 27.6, 20.9 ppm; IR (film): <math>\tilde{\nu}_{max}</math> = 1702, 1585, 1558, 1540, 1456, 1340, 1263, 1232 cm<sup>-1</sup>; HRMS (ESI TOF) (<math>m/z</math>): calcd for C<sub>32</sub>H<sub>27</sub>O<sub>10</sub><sup>+</sup>: 571.1599 [M+H]<sup>+</sup>; found: 571.1593</p> <p><b>4:</b> <math>R_f</math> = 0.40 (CH<sub>2</sub>Cl<sub>2</sub>/MeOH 10:1); <sup>1</sup>H NMR (500 MHz, CDCl<sub>3</sub>): <math>\delta</math> = 6.55 (2 H, d, <math>J</math> = 2.5 Hz), 6.49 (2 H, d, <math>J</math> = 2.5 Hz), 3.88 (6 H, s), 3.74 (6 H, s), 3.68 (2 H, br), 3.08 (2 H, ddd, <math>J</math> = 17.5, 7.5, 7.5 Hz), 2.75 (2 H, dd, <math>J</math> = 24.0, 4.5 Hz), 2.33–2.25 ppm (4 H, m); <sup>13</sup>C NMR (125 MHz, CDCl<sub>3</sub>): <math>\delta</math> = 195.3, 187.2, 180.0, 163.9, 160.7, 151.5, 134.9, 134.6, 114.9, 105.2, 101.4, 56.2, 55.8, 34.0, 32.4, 25.2 ppm; IR (film): <math>\tilde{\nu}_{max}</math> = 1780, 1698, 1661, 1590, 1461, 1320, 1255, 1212, 909, 731 cm<sup>-1</sup>; HRMS (ESI TOF) (<math>m/z</math>): calcd for C<sub>32</sub>H<sub>27</sub>O<sub>10</sub><sup>+</sup>: 571.1599 [M+H]<sup>+</sup>; found: 571.1595</p> <p><b>5:</b> <math>R_f</math> = 0.71 (CH<sub>2</sub>Cl<sub>2</sub>/MeOH 10:1); <sup>1</sup>H NMR (500 MHz, CDCl<sub>3</sub>): <math>\delta</math> = 16.28 (1 H, s), 15.02 (1 H, s), 6.61 (1 H, d, <math>J</math> = 2.0 Hz), 6.31 (1 H, d, <math>J</math> = 2.0 Hz), 6.19 (1 H, d, <math>J</math> = 2.5 Hz), 5.90 (1 H, d, <math>J</math> = 2.5 Hz), 3.97 (3 H, s), 3.93 (3 H, s), 3.56 (3 H, s), 3.43 (3 H, s), 2.82–2.80 (1 H, m), 2.74–2.70 (1 H, m), 2.60–2.57 (5 H, m), 2.26–2.23 (1 H, m), 2.19–2.13 (1 H, m), 2.12–2.09 ppm (1 H, m); <sup>13</sup>C NMR (125 MHz, CDCl<sub>3</sub>): <math>\delta</math> = 202.9, 197.6, 188.1, 184.1, 164.9, 162.0, 161.9, 161.0, 160.7, 139.6, 137.9, 134.6, 125.2, 115.0, 109.8, 108.0, 104.3, 103.8, 102.2, 98.2, 92.0, 82.0, 56.4, 56.2, 55.9, 55.0, 39.6, 38.7, 38.2, 30.4, 29.3, 25.3 ppm; IR (film): <math>\tilde{\nu}_{max}</math> = 1710, 1601, 1558, 1385, 1320, 1207, 1153, 1044 cm<sup>-1</sup>; HRMS (ESI TOF) (<math>m/z</math>): calcd for C<sub>32</sub>H<sub>29</sub>O<sub>10</sub><sup>+</sup>: 573.1755 [M+H]<sup>+</sup>; found: 573.1742</p>
---

**Keywords:** cascade reactions · dimerization · natural products · radicals · synthetic methods

[1] S. F. Brady, M. P. Singh, J. E. Janso, J. Clardy, *Org. Lett.* **2000**, 2, 4047–4049.

[2] In a series of papers that were intriguing but lacking in details, the Shibata group reported on their investigations in this field, which included both the isolation of and chemical interconversions between some of these natural products and related compounds, see: a) N. Takeda, S. Seo, Y. Ogihara, U. Sankawa, I. Iitaka, I. Kitagawa, S. Shibata, *Tetrahedron* **1973**, 29, 3703–3719; b) Y. Ogihara, N. Kobayashi, S. Shibata, *Tetrahedron Lett.* **1968**, 1881–1886; c) S. Seo, U. Sankawa, S. Shibata, *Tetrahedron Lett.* **1972**, 731–734; d) S. Shibata, *Pure Appl. Chem.* **1972**, 33, 109–127; e) S. Seo, U. Sankawa, Y. Ogihara, Y. Iitaka, S. Shibata,

- Tetrahedron* **1973**, 29, 3721–3726; f) D.-M. Yang, U. Sankawa, Y. Ebizuka, S. Shibata, *Tetrahedron* **1976**, 32, 333–335.
- [3] P. Sedmera, M. Podojil, J. Vokoun, V. Betina, P. Nemec, *Folia Microbiol.* **1978**, 23, 64–67.
- [4] B. Franck, R. Chahin, H.-G. Eckert, R. Langenberg, V. Radtke, *Angew. Chem.* **1975**, 87, 846–847; *Angew. Chem. Int. Ed. Engl.* **1975**, 14, 819–820.
- [5] Clardy and co-workers speculated on the biosynthetic origins of cytoskyrin A as following a redox path from monomeric 6-methyl-1,3,8-trihydroxyanthraquinone (emodin, see reference [1]). This type of dimerization had been hinted at earlier by the Shibata group (see reference [2e]).
- [6] Polysubstituted examples of this cage structure have been described previously: a) J. A. Beisler, J. V. Silverton, A. Penttila, D. H. S. Horn, H. M. Fales, *J. Am. Chem. Soc.* **1971**, 93, 4850–4855; b) K. Hirao, Y. Ohuchi, O. Yonemitsu, *J. Chem. Soc. Chem. Commun.* **1982**, 99–100.
- [7] F. M. Hauser, S. Chakrapani, W. P. Ellenberger, *J. Org. Chem.* **1991**, 56, 5248–5250.
- [8] a) D. Momose, K. Iguchi, T. Sugiyama, Y. Yamada, *Tetrahedron Lett.* **1983**, 24, 921–924; b) S. K. Bagal, R. M. Adlington, R. Marquez, A. R. Cowley, J. E. Baldwin, *Tetrahedron Lett.* **2003**, 44, 4993–4996.
- [9] CCDC-274275 (**4**), -274271 (**5**), and -274272 (**3**) contain the supplementary crystallographic data for this paper. These data can be obtained free of charge from the Cambridge Crystallographic Data Centre via [www.ccdc.cam.ac.uk/data\\_request/cif](http://www.ccdc.cam.ac.uk/data_request/cif).
- [10] The high overall yield for this cascade reflects the higher efficiency by which the final product (**1**) can be purified by chromatography, as opposed to the intermediate compounds (**3** or **2**) whose enolic nature makes their isolation more tedious.
- [11] O. Ermer, *Angew. Chem.* **1983**, 95, 251–252; *Angew. Chem. Int. Ed. Engl.* **1983**, 22, 251–252. We thank Professor Scott Rychnovsky for pointing out this reference to us.
- [12] The NMR spectroscopic analysis of compound **3** included <sup>1</sup>H and <sup>13</sup>C NMR data as well as COSY and HMQC correlations, which can be found in the Supporting Information.
- [13] a) J. D. Dunitz, G. Filippini, A. Gavezzotti, *Helv. Chim. Acta* **2000**, 83, 2317–2335; b) J. D. Dunitz, J. Bernstein, *Acc. Chem. Res.* **1995**, 28, 193–200, and references therein. We thank Professor Jack Dunitz for pointing out these articles to us and for his stimulating comments.
- [14] The X-ray measurements were initially performed at room temperature and the crystal structure was solved and refined in the centrosymmetric space group *C2/c* with *Z* = 4, following the general conventions and statistical analysis of data ( $|E^2 - 1| = 0.91$ ). Accordingly, the molecules of **3** were observed to reside on (average) crystallographic twofold axes. The distance between the carbon atoms C9 and C12', however, was as short as 2.37 (2) Å, which was far smaller than the expected van der Waals sum of 3.5 Å. Furthermore, the anisotropic temperature factor ellipsoids of both these atoms were distinctly elongated along their line of separation, suggesting that one Michael addition reaction could have taken place, resulting in bond formation between C9 and C12' and leading to the nonsymmetrical structure **3**, which could exist in dynamic equilibrium with its identical "regioisomer" (**3'**, Figure 4b). Subsequent crystal structure solution and refinement in the lower noncentrosymmetric space group *Cc*,<sup>[15]</sup> gave a slightly nonsymmetrical molecular structure with C9–C12' and C9'–C12 distances of 2.24(2) and 2.52(1) Å, respectively. Interestingly, when the same crystal was subjected to low-temperature X-ray measurements (123 K), these bond lengths diverged even further, as revealed by the values of 1.91(2) and 2.81(2) Å, computed by structure solution and refinement in *Cc*. When the *C2/c* space group was used the C9–C12' distance was approximately the same as the room-temperature distance of 2.37 Å (2). These distances were
- even more drastically different [1.66(2) and 2.95(2) Å, respectively] in *Cc* when the atoms were refined isotropically. Thus, apparently partial dynamic ordering of the crystal structure occurs on cooling. Interestingly, while both the secododecahedrane<sup>[11]</sup> and the present examples involve carbon atoms at close proximity to each other, in the former case the X-ray analysis revealed a bond, whereas in the latter case it missed a bond.
- [15] We thank Professor O. Ermer for suggesting that we revert to this space group (*Cc*) and for critically reviewing our conclusions regarding this anomalous X-ray crystallographic analysis.